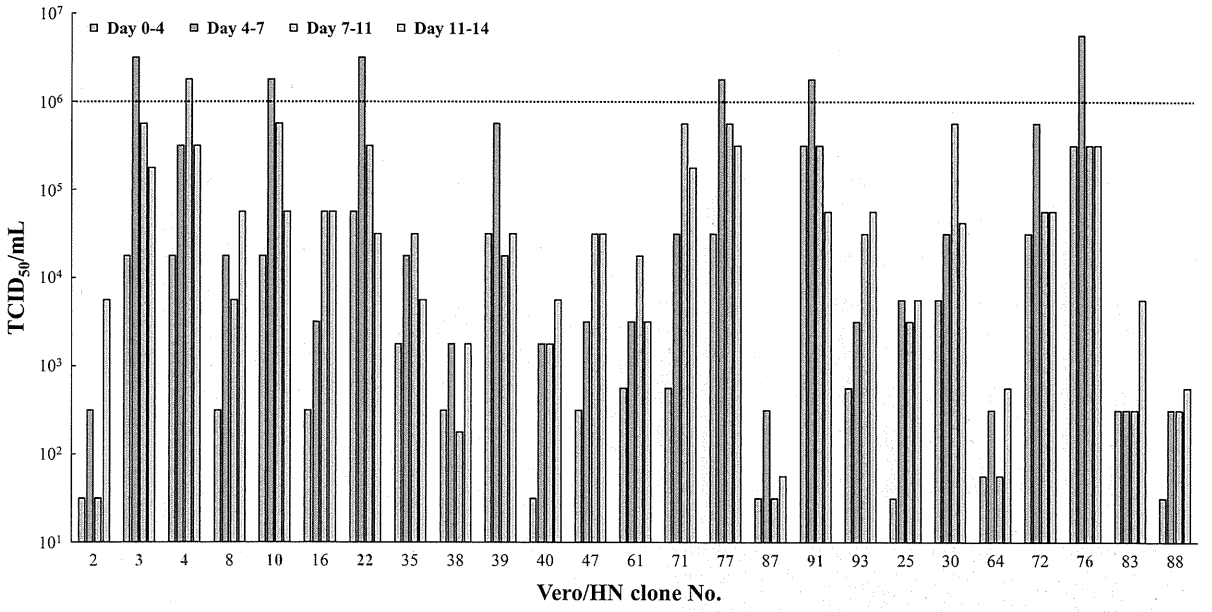

図 3 候補株 25 クローンでの rhPIV2ΔHN-EGFP 産生能比較

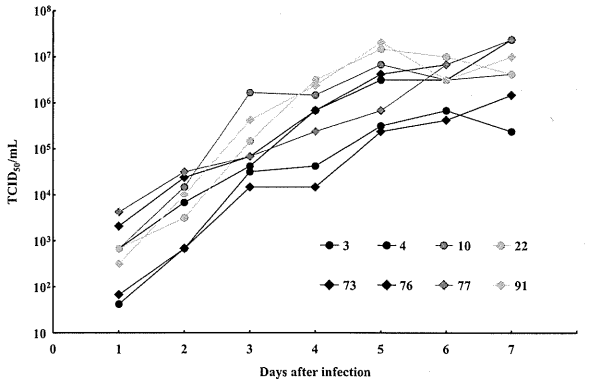

図4 rhPIV2ΔHN-EGFPタイターの経時変化

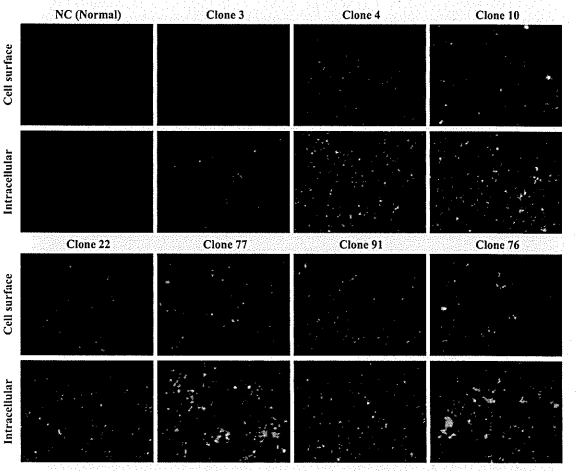

図5 間接蛍光抗体法によるHN蛋白質の検出

(4) Vero/HN 株の免疫蛍光染色によるHN 抗原の発現

効率的に感染性ウイルスを産生したVero/HNの7 株におけるHN 抗原の発現を確認するため、細胞表面及び細胞内を抗HN 抗体で免疫蛍光染色した。その結果、いずれのクローンでも細胞表面、細胞内ともにHN 抗原の発現が確認された。ウイルス産生量が低かったクローン3でのHN発現レベルが若干低かったが、高生産性クローン間でのHN発現に顕著な差は認められなかった(図5)。

D. 考察

今回、rPIV2ΔHN 株を効率的に産生可能な組換えVero 細胞クローンが得られたが、これは pCXneoHN発現ベクターをVero 細胞に導入する際の、トランスフェクション試薬を前回のFugeneからLipofectamine 2000に変更することにより、 HN遺伝子導入効率が向上したことによると考えられる。これにより、PCR陽性クローン取得率が格段に向上すると同時に、HN発現レベルも上昇したクローンを得ることができた。各クローンでのrPIV2ΔHN-EGFPウイルスタイターは、HN発現が弱い領域ではその発現レベルとの相関が見られるが、発現が強い株間では相関が見られないことから、ある発現レベル以上では、ウイルス産生に差がないものと考えられる。

E. 結論

HN遺伝子導入Vero細胞のクローニングを行い、PCRおよびrhPIV2ΔHN-EGFP増殖性を指標にスクリーニングすることにより、ウイルス高生産株を7クローン得ることができた。最も高い生産性を示したクローンでは、10^7 TCID50/mL以上のタイターが得られており、実用化可能なレベルに達していると思われる。今後、樹立した細胞を用いて、実際に結核菌抗原遺伝子が組み込まれたΔHN ウイルスをラボスケールで製造し、サルでの実験等に供給することが急務である。

G. 研究発表

1. 論文発表

(1) Watanabe K, Matsubara A, Kawano M, Mizuno S, Okamura T, Tsujimura Y, Inada H, Nosaka T, Matsuo K, Yasutomi Y. Recombinant Ag85B vaccine by taking advantage of characteristics of human parainfluenza type 2 virus vector showed Mycobacteria-specific immune responses by intranasal immunization. Vaccine, 32(15):1727-35 (2014).

(2) Tsujimura Y, Inada H, Yoneda M, Fujita T, Matsuo K, Yasutomi Y. Effects of mycobacteria major secretion protein, Ag85B, on allergic inflammation in the lung. PLoS One 9(9):e106807 (2014).

2. 学会発表

(1) 水野悟、加藤誠一、相馬祥吾、保富康宏、松尾和浩. 新規結核ワクチン候補: SOCS1 アンタゴニスト発現型組換えBCGの評価. 第18回日本ワクチン学会学術集会, 2014年, 福岡

H. 知的財産権の出願・登録状況

なし

研究成果の刊行に関する一覧表

（平成２６年度）

研究成果の刊行に関する一覧表

書籍

著者氏名	論文タイトル名	書籍全体の編集者名	書　籍　名	出版社名	出版地	出版年	ページ
鈴木英彦、<u>國澤純</u>	粘膜免疫システムの多面的機能を応用したワクチン開発の現状と未来	米田悦啓、堤康央、石井健	*The Frontiers in Life Sciences*「*生命科学からの創薬へのイノベーション*」	南山堂	東京	2014	57-62

雑誌

発表者氏名	論文タイトル名	発表誌名	巻号	ページ	出版年
Okabayashi S, Shimozawa N, Yasutomi Y, Yanagisawa K, Kimura N.	Diabetes mellitus accelerates Aβ pathology in brain accompanied by enhanced GAβ generation in nonhuman primates	*PLos One*			印刷中
Onishi M, Ozasa K, Kobiyama K, Ohata K, Kitano M, Taniguchi K, Homma T, Kobayashi M, Sato A, Katakai Y, Yasutomi Y, Wijaya E|, Igarashi Y, Nakatsu N, Ise W, Inoue T, Yamada H, Vandenbon A|, Standley DM|, Kurosaki T, Coban C, Aoshi T, Kuroda E, Ishii KJ.	Hydroxypropyl-β-cyclodextrin spikes local inflammation that induce Th2 and Tfh responses to the coadministered antigen	*J.Immunol*			印刷中
Watanabe K., Matsubara A, Kawano M, Mizuno S, Okamura T, Tsujimura Y, Inada H, Nosaka T, Matsuo K. and Yasutomi Y.	Recombinant Ag85B vaccine by taking advantage of characteristics of human parainfluenza type 2 virus vector showed Mycobacteria-specific immune responses by intranasal immunization.	*Vaccine*	32	1727-1735	2014
Kobiyama K., Aoshi T., Narita H., Kuroda E., Hayashi M., Tetsutani K., Koyama S., Mochizuki S., Sakurai K., Katakai Y., Yasutomi Y., Saijo S., Iwakura Y., Akira S., Coban C. and Ishii KJ.	A non-agonistic Dectin-1 ligand transforms CpG into a multitask nano-particulate TLR9 agonist.	*Proc. Natl. Acad Sci.USA*	111	3086-3091	2014
Tsujimura Y, Inada H, Yoneda M, Fujita T, Matsuo K. and Yasutomi Y.	Effects of Mycobacteria major secretion protein, Ag85B, on allergic inflammation in the lung.	*Plos One*	9 (9)	e106807	2014
Saito N, Chono H, Shibata H, Ageyama N, Yasutomi Y. and Mineo J.	CD4(+) T cells modified by the endoribonuclease MazF are safe and can persist in SHIV-infected rhesus macaques.	*Mol. Ther. Nucleic Acids*	E-pub		2014
Machino-Ohtsuka T, Tajiri K, Kimura T, Sakai S, Sato A, Yoshida T, Hiroe M, Yasutomi Y, Aonuma K, Imanaka-	Tenascin-C aggravates autoimmune myocarditis via dendritic cell activation and Th17 cell differentiation.	*J.Am.Heart Assoc.*	E-pub		2014

Yoshida K.					
Tachibana SI, Kawai S, Katakai Y, Takahashi H, Nakade T, Yasutomi Y, Horii T, Tanabe K.	Contrasting infection susceptibility of the Japanese macaques and cynomolgus macaques to closely related malaria parasites, Plasmodium vivax and Plasmodium cynomolgi.	*Parasitol. Int.*	E-pub		2014
Fukuyama Y., Yuki Y., Katakai Y., Harada N., Takahashi H., Takeda S., Mjima M., Joo S., Kurokawa S., Sawada S., Shibata H., Park EJ., Fujihashi K., Briles DE., Yasutomi Y., Tsukada H., Akiyoshi K. and Kiyono H	Nanogel-based pneumococcal surface protein A nasal vaccine induces microRNA-associated Th17 cell responses with neutralizing antibodies against Streptococcus pneumonia in macaques.	*Mucosal Immunology*	E-pub		2015
Ohtsuka J, Fukumura M, Tsurudome M, Hara K, Nishio M, Kawano M, Nosaka T.	Vero/BC-F: an efficient packaging cell line stably expressing F protein to generate single round-infectious human parainfluenza virus type 2 vector.	*Gene Ther*	21	775-784	2014
Kihira S, Uematsu J, Kawano M, Itoh A, Ookohchi A, Satoh S, Maeda Y, Sakai K, Yamamoto H, Tsurudome M, O'Brien M, Komada H.	Ribavirin inhibits human parainfluenza virus type 2 replication in vitro.	*Microbiol Immunol*	58	628-635	2014
Yano T, Maeda C, Akachi S, Matsuno Y, Yamadera M, Kobayashi T, Nagai Y, Iwade Y, Kusuhara H, Katayama M, Fukuda M, Nakagawa Y, Naraya S, Takahashi H, Hiraoka M, Yamauchi A, Nishinaka T, Amano H, Yamaguchi T, Ochiai H, Ihara T, Matsuzaki Y.	Phylogenic analysis and seroprevalence of influenza C virus in Mie Prefecture, Japan in 2012.	*Jpn J Infect Dis.*	67	127-131	2014
矢野拓弥、落合仁、庵原俊昭	三重県における急性呼吸器症状を呈した小児から検出されたコロナウイルス(HCoV-OC43)	*感染症学雑誌*	88 (5)	708-710	2014
矢野拓弥、落合仁、渡辺正博、庵原俊昭	呼吸器症状を呈した小児から検出されたヒトボカウイルスの流行疫学および遺伝子系統樹解析(2010～2013年)	*小児感染免疫*	26 (3)	369-375	2014
Yano T, Fukuda M,	Epidemiological investig	*Jpn J Infect Di*	67	506-508	2014

Maeda C, Akachi S, Matsuno Y, Yamadera M, Kobayashi A, Nagai Y, Kusuhara H, Kobayashi T, Amano H, Nishinaka T, Ochiai H, Watanabe M, Nakamura H, Suga S, Ihara T:	ation and seroprevalence of human parainfluenza virus in Mie Prefcture in Japan during 2009-2013.	*s.*			
Koo CX, Kobiyama K, Shen YJ, LeBert N, Ahmad S, Khatoo M, Aoshi T, Gasser S, Ishii KJ.	RNA Polymerase III Regulates Cytosolic RNA:DNA Hybrids and Intracellular MicroRNA Expression	*J Biol Chem*			2015
Temizoz B, Kuroda E, Ohata K, Jonai N, Ozasa K, Kobiyama K, Aoshi T, Ishii KJ.	TLR9 and STING agonists synergistically induce innate and adaptive type II IFN.	*Eur J Immunol*			2014
Natsuaki Y, Egawa G, Nakamizo S, Ono S, Hanakawa S, Okada T, Kusuba N, Otsuka A, Kitoh A, Honda T, Nakajima S, Tsuchiya S, Sugimoto Y, Ishii KJ, Tsutsui H, Yagita H, Iwakura Y, Kubo M, Ng Lg, Hashimoto T, Fuentes J, Guttman-Yassky E, Miyachi Y, Kabashima K.	Perivascular leukocyte clusters are essential for efficient activation of effector T cells in the skin.	*Nat Immunol*	15(11)	1064-9	2014
Piao Z, Akeda Y, Takeuchi D, Ishii KJ, Ubukata K, Briles DE, Tomono K, Oishi K.	Protective properties of a fusion pneumococcal surface protein A (PspA) vaccine against pneumococcal challenge by five different PspA clades in mice.	*Vaccine.*	32 (43)	5607-13	2014
Uraki R, Das SC, Hatta M, Kiso M, Iwatsuki-Horimoto K, Ozawa M, Coban C, Ishii KJ, Kawaoka Y.	Hemozoin as a novel adjuvant for inactivated whole virion influenza vaccine.	*Vaccine.*	32 (41)	5295-300	2014
Mizukami T, Momose H, Kuramitsu M, Takizawa K, Araki K, Furuhata K, Ishii KJ,	System vaccinology for the evaluation of influenza vaccine safety by multiplex gene	*PLoS One.*	9(7)	e101835.	2014

Hamaguchi I, Yamaguchi K.	detection of novel biomarkers in a preclinical study and batch release test.				
Hemmi M, Tachibana M, Tsuzuki S, Shoji M, Sakurai F, Kawabata K, Kobiyama K, Ishii KJ, Akira S, Mizuguchi H.	The early activation of CD8+ T cells is dependent on type I IFN signaling following intramuscular vaccination of adenovirus vector.	*Biomed Res Int.*	2014	158128	2014
Yagi M, Bang G, Tougan T, Palacpac NM, Arisue N, Aoshi T, Matsumoto Y, Ishii KJ, Egwang TG, Druilhe P, Horii T.	Protective epitopes of the Plasmodium falciparum SERA5 malaria vaccine reside in intrinsically unstructured N-terminal repetitive sequences.	*LoS One.*	9(6)	e98460.	2014
Zhao H, Aoshi T, Kawai S, Mori Y, Konishi A, Ozkan M, Fujita Y, Haseda Y, Shimizu M, Kohyama M, Kobiyama K, Eto K, Nabekura J, Horii T, Ishino T, Yuda M, Hemmi H, Kaisho T, Akira S, Kinoshita M, Tohyama K, Yoshioka Y, Ishii KJ, Coban C.	Olfactory plays a key role in spatiotemporal pathogenesis of cerebral malaria.	*Cell Host Microbe.*	15(5)	551-63	2014
Onishi M, Kitano M, Taniguchi K, Homma T, Kobayashi M, Sato A, Coban C, Ishii KJ.	Hemozoin is a potent adjuvant for hemagglutinin split vaccine without pyrogenicity in ferrets.	*Vaccine.*	32(25)	3004-9	2014
Imanishi T, Ishihara C, Badr Mel S, Hashimoto-Tane A, Kimura Y, Kawai T, Takeuchi O, Ishii KJ, Taniguchi S, Noda T, Hirano H, Brombacher F, Barber GN, Akira S, Saito T.	Nucleic acid sensing by T cells initiates Th2 cell differentiation.	*Nat Commun.*	5	3566	2014
Lam AR, Le Bert N, Ho SS, Shen YJ, Tang ML, Xiong GM, Croxford JL, Koo CX, Ishii KJ, Akira	RAE1 ligands for the NKG2D receptor are regulated by STING-dependent DNA sensor	*Cancer Res.*	74(8)	2193-203	2014

S, Raulet DH, Gasser S.	pathways in lymphoma.				
J. Kunisawa, M. Arita, T. Hayasaka, T. Harada, R. Iwamoto, R. Nagasawa, S. Shikata, T. Nagatake, H. Suzuki, E. Hashimoto, Y. Kurashima, Y. Suzuki, H. Arai, M. Setou, and H. Kiyono	Dietary ω3 fatty acid exerts anti-allergic effect through the conversion to 17,18-epoxyeicosatetraenoic acid in the gut	*Scientific Reports*			2015 (in press)
Y. Kurashima, H. Kiyono, and J. Kunisawa	Pathophysiological role of extracellular purinergic mediators in the control of intestinal inflammation	*Mediators of Inflammation*			2015 (in press)
J. Kunisawa and H. Kiyono	Vitamins mediate immunological homeostasis and diseases at the surface of the body	*Endocr Metab Immune Disord Drug Targets*			2015 (in press)
Y. Goto, T. Obata, J. Kunisawa, S. Sato, I. I. Ivanov, A. Lamichhane, N. Takeyama, M. Kamioka, M. Sakamoto, T. Matsuki, H. Setoyama, A. Imaoka, S. Uematsu, S. Akira, S. E. Domino, P. Kulig, B. Becher, J. Renauld, C. Sasakawa, Y. Umesaki, Y. Benno, and H. Kiyono	Innate lymphoid cells govern intestinal epithelial fucosylation	*Science*	345	1254009	2014
A. Sato, A. Suwanto, M. Okabe, S. Sato, T. Nochi, T. Imai, N. Koyanagi, J. Kunisawa, Y. Kawaguchi, and H. Kiyono	Vaginal memory T cells induced by intranasal vaccination are critical for protective T cell recruitment and prevention of genital HSV-2 disease	*J Virol*	88	13699-708	2014
J. Kunisawa, E. Hashimoto, A. Inoue, R. Nagasawa, Y. Suzuki, I.Ishikawa, S. Shikata, M. Arita, J. Aoki, and H. Kiyono	Regulation of intestinal IgA responses by dietary palmitic acid and its metabolism	*J Immunol*	193	1666-1671	2014
Y. Kurashima, T. Amiya, K. Fujisawa, N. Shibata, Y. Suzuki, Y. Kogure, E. Hashimoto, A. Otsuka, K. Kabashima, S. Sato, T. Sato, M. Kubo, S. Akira, K. Miyake, J. Kunisawa and H. Kiyono	The enzyme Cyp26b1 mediates inhibition of mast cell activation by fibroblasts to maintain skin-barrier homeostasis	*Immunity*	40	530-41	2014
長竹貴広、國澤　純	腸管組織における多元的免疫制御システムと	*医学のあゆみ*			2015 (印刷

	食物アレルギー				中)
鈴木英彦、<u>國澤純</u>	粘膜免疫の特異性に着目したワクチンマテリアルの開発	*感染・炎症・免疫*			2015 (印刷中)
鈴木英彦、<u>國澤　純</u>	CD11b 陽性 IgA 産生細胞の誘導と機能	*臨床免疫・アレルギー科*	62	552-556	2014
倉島　洋介、佐藤研、清野　宏、<u>國澤純</u>	DAMPs によるマウス細胞の活性化と疾患	*臨床免疫・アレルギー科*	62	675-679	2014
長竹　貴広、<u>國澤　純</u>	脂質を介した腸管免疫システムの制御	*医学のあゆみ*	248	1019-1024	2014
近藤　昌夫、<u>國澤　純</u>	上皮細胞を標的とした創薬研究の新展開	*薬学雑誌*	134	613	2014
鈴木　英彦、近藤　昌夫、八木　清仁、清野宏、<u>國澤　純</u>	微生物の有する粘膜組織指向性を用いた粘膜ワクチンデリバリー開発への展望	*薬学雑誌*	134	629-634	2014
高里　良宏、倉島　洋介、清野　宏、<u>國澤純</u>	抑制型免疫システムを利用した次世代型抗アレルギーワクチンの開発	*Bioindustry*	6	55-60	2014

PLOS | ONE

RESEARCH ARTICLE

Diabetes Mellitus Accelerates Aβ Pathology in Brain Accompanied by Enhanced GAβ Generation in Nonhuman Primates

Sachi Okabayashi[1,2], Nobuhiro Shimozawa[1], Yasuhiro Yasutomi[1], Katsuhiko Yanagisawa[3], Nobuyuki Kimura[1,3]*

1 Tsukuba Primate Research Center, National Institute of Biomedical Innovation, 1–1 Hachimandai, Tsukuba-shi, Ibaraki, 305–0843, Japan, **2** The Corporation for Production and Research of Laboratory Primates, 1–1 Hachimandai, Tsukuba-shi, Ibaraki, 305–0843, Japan, **3** Section of Cell Biology and Pathology, Department of Alzheimer's Disease Research, Center for Development of Advanced Medicine for Dementia, National Center for Geriatrics and Gerontology (NCGG), Gengo 35, Moriika, Obu, Aichi, 474–8511, Japan

* kimura@ncgg.go.jp

OPEN ACCESS

Citation: Okabayashi S, Shimozawa N, Yasutomi Y, Yanagisawa K, Kimura N (2015) Diabetes Mellitus Accelerates Aβ Pathology in Brain Accompanied by Enhanced GAβ Generation in Nonhuman Primates. PLoS ONE 10(2): e0117362. doi:10.1371/journal.pone.0117362

Academic Editor: Yoshitaka Nagai, National Center of Neurology and Psychiatry, JAPAN

Received: July 20, 2014

Accepted: December 21, 2014

Published: February 12, 2015

Data Availability Statement: All relevant data are within the paper and its Supporting Information files.

Funding: This study was supported by The Research Funding for Longevity Sciences (25-20) from National Center for Geriatrics and Gerontology (NCGG), Japan. The funders had no role in study design, data collection and analysis, decision to publish, or preparation of the manuscript.

Competing Interests: The authors have declared that no competing interests exist.

Abstract

Growing evidence suggests that diabetes mellitus (DM) is one of the strongest risk factors for developing Alzheimer's disease (AD). However, it remains unclear why DM accelerates AD pathology. In cynomolgus monkeys older than 25 years, senile plaques (SPs) are spontaneously and consistently observed in their brains, and neurofibrillary tangles are present at 32 years of age and older. In laboratory-housed monkeys, obesity is occasionally observed and frequently leads to development of type 2 DM. In the present study, we performed histopathological and biochemical analyses of brain tissue in cynomolgus monkeys with type 2 DM to clarify the relationship between DM and AD pathology. Here, we provide the evidence that DM accelerates Aβ pathology *in vivo* in nonhuman primates who had not undergone any genetic manipulation. In DM-affected monkey brains, SPs were observed in frontal and temporal lobe cortices, even in monkeys younger than 20 years. Biochemical analyses of brain revealed that the amount of GM1-ganglioside-bound Aβ (GAβ)—the endogenous seed for Aβ fibril formation in the brain—was clearly elevated in DM-affected monkeys. Furthermore, the level of Rab GTPases was also significantly increased in the brains of adult monkeys with DM, almost to the same levels as in aged monkeys. Intraneuronal accumulation of enlarged endosomes was also observed in DM-affected monkeys, suggesting that exacerbated endocytic disturbance may underlie the acceleration of Aβ pathology due to DM.

Introduction

Alzheimer's disease (AD) is a progressive neurological disorder that is histopathologically characterized by the formation of senile plaques (SPs) and neurofibrillary tangles (NFTs) [1, 2]. It is widely accepted that β-amyloid protein (Aβ), the major component of SPs, is a key molecule

underlying AD pathogenesis [3, 4]. Several epidemiological/clinical studies have shown that diabetic mellitus (DM) patients are significantly more likely to develop cognitive dysfunction and exhibit increased susceptibility to AD [5–9], in consistent with the original Rotterdam study [10]. Recent findings also showed that there are several pathogenic connections between AD and DM patient brains, such as brain inflammation, mitochondrial dysfunction, and defective neuronal insulin signaling [11]. Insulin resistance causes alteration in GSK3β kinase signaling pathway as observed in AD brains, and it is also associated with an AD-like pattern of reduced cerebral glucose metabolic rate in brain [12, 13]. Moreover, accumulating evidences showed that the experimental induction of DM enhanced AD pathology even in rodents [14–25]. However, it remains unclear how DM physiologically accelerates AD pathology in the brain.

With advancing age, both SPs and NFTs occur spontaneously in brains of cynomolgus monkeys [26, 27]. In addition, the amino acid sequence of Aβ of cynomolgus monkeys is completely consistent with that of humans [28]. These advantages make this species a useful model to study age-dependent AD pathophysiology. As with humans, obesity occasionally occurs in adult, middle-aged monkeys, and it can result in the development of type 2 DM [29, 30]. Similar to the case of humans, these monkeys have a period of insulin resistance and hyperinsulinemia before developing overt DM, which is then accompanied by deficiency in pancreatic insulin production [29–31]. The pathological changes that occur in the pancreatic islets of aged monkeys are also similar to those seen in human diabetics, including the deposition of islet amyloid polypeptide (IAPP) [29–31]. In addition, gestational diabetes has been also reported in female cynomolgus monkeys [29–31]. Thus, cynomolgus monkeys are a useful species to investigate not only age-dependent AD lesions but also the relationship between DM and AD pathology.

Here, we report that DM enhances the generation of GM1-ganglioside-bound Aβ (GAβ) to accelerate SP deposition in cynomolgus monkey brains. GAβ was previously identified as the endogenous seed for Aβ fibril formation in the brain, and its generation is enhanced by endocytic disturbance, which is considered to be involved in early-stage AD pathology [32–34]. In DM-affected adult monkeys, the level of Rab GTPases in the brain was obviously increased as compared to normal adult monkeys, and intraneuronal endosomes were apparently enlarged. These findings suggest that DM exacerbates age-dependent endocytic disturbance, which then may lead to accelerate Aβ pathology via enhanced GAβ generation.

Materials and Methods

Animals

Forty-one cynomolgus monkey (*Macaca fascicularis*) brains were used in this study. Of these, six brains were from young monkeys (age: 6 and 7 years); six were from normal adult monkeys (age: 17, 18, 19, and 20 years); nine were from DM-affected adult monkeys (age: 17, 18, 19, and 20 years); ten were from normal aged monkeys (age: 24, 25, 26, and 28 years); and ten were from DM-affected aged monkeys (age: 24, 25, 26, and 28 years). The frontal and temporal lobes were used for immunohistochemical studies. The cerebral cortices of 12 monkeys were used for dot blot analyses. Of these 12, 3 were from young monkeys (age: 6 years [N = 2] and 7 years [N = 1]); 3 were from normal adult monkeys (age: 18 years, 19 years, and 20 years [N = 1 each]); 3 were from DM-affected adult monkeys (age: 18 years, 19 years, and 20 years [N = 1 each]); and 3 were from normal aged monkeys (age: 26 years [N = 2] and 28 years [N = 1]). The cerebral cortices of 12 female monkeys were used for Western blot analyses. Of these 12, 3 were from young monkeys (age: 7 years [N = 3]); 3 were from normal adult monkeys (age: 18 years, 19 years, and 20 years [N = 1 each]); 3 were from DM-affected adult monkeys (age: 18 years, 19 years, and 20 years [N = 1 each]); and 3 were from normal aged monkeys (age: 25 years and 26 years [N = 2]). The cerebral cortices of 14 female monkeys were used for

Aβ ELISA. Of these 12, 4 were from young monkeys (age: 7 years [N = 4]); 3 were from normal adult monkeys (age: 18 years, 19 years, and 20 years [N = 1 each]); 3 were from DM-affected adult monkeys (age: 18 years, 19 years, and 20 years [N = 1 each]); and 4 were from normal aged monkeys (age: 24 years [N = 3], and 25 years [N = 1]). All brains were obtained from the Tsukuba Primate Research Center (TPRC), National Institute of Biomedical Innovation (NIBIO), Japan. Monkeys in the TPRC are reared in individual cages (0.5 m wide × 0.8 m high × 0.9 m deep; stain-less steel mesh). The breeding rooms are rectangular, and the individual cages are installed on the long sides of the room. Each room contains at least 90 cages. Therefore, monkeys can always make visual, auditory and olfactory contact with their roommates. Ambient temperature in the rooms is kept about 25°C, and humidity is set at 50% to 60%. The air is replaced 12 times hourly. Monkeys are provided with 100 g of apples in the morning, and 70 g of commercial food (Type AS; Oriental Yeast Co., Ltd., Tokyo, Japan) is given to them twice in the afternoon. Water is available ad libitum. Every morning their health status (e.g., viability, appetite, fur-coat appearance) was monitored by experienced animal technicians. When any abnormality is found, a veterinarian examines the monkey promptly and applies the appropriate treatment. Moreover, the monkeys are medically examined under anesthesia (ketamine hydrochloride) at least once every 2 y. The medical examination consists of body weight measurement, tuberculin test, blood sample, stool test, examination of the fundus, and a medicated bath. The maintenance of animals was conducted according to the rules for animal care of the TPRC at NIBIO for the care, use, and biohazard countermeasures of laboratory animals [35]. This study was carried out in strict accordance with the recommendations in the Animal Care and Use Committee of the NIBIO, Japan. The protocol was approved by the Committee on the Ethics of Animal Experiments of the NIBIO (DS17-001R1). When the monkey presents clinical symptoms by injury or illness and it could not expect recovery from pain or morbidity, it is judged as poor prognosis. In the present study, the animals used in this study died of natural causes were euthanized when they reached endpoints determined as poor prognosis. All DM-affected monkeys were also sacrificed because of poor prognosis. For euthanasia, the monkeys were deeply anesthetized with a lethal dose of pentobarbital, and all efforts were made to minimize suffering.

Antibodies

In this study, we used the following antibodies: mouse monoclonal anti-dynein heavy chain (DHC) (Sigma, Saint Louis, MO); mouse monoclonal anti-dynein intermediate chain (DIC) (Millipore, Temecula, CA); mouse monoclonal anti- GAβ antibody (4396C) (22); mouse monoclonal kinesin light chain (KLC) (Santa Cruz Biotechnology, Santa Cruz, CA); mouse monoclonal anti-neprilysin (NEP; DAKO, Glostrup, Denmark); mouse monoclonal anti-phosphorylated tau antibody (AT8; Innogenetics, Gent, Belgium); mouse monoclonal anti-Rab5 antibody (Rab5m; Santa Cruz Biotechnology); rabbit polyclonal anti-Aβ antibody (IBL); rabbit polyclonal anti-full-length β-amyloid precursor protein (APP) antibody (IBL); rabbit polyclonal anti-Cathepsin D (CatD; Cell Signaling Technology, Danvers, MA); rabbit polyclonal anti-kinesin heavy chain (KHC) (Sigma); rabbit polyclonal anti-LC3 (Novus Biologicals, Littleton, CO); rabbit polyclonal anti-Rab5 antibody (Santa Cruz Biotechnology); rabbit polyclonal anti-Rab7 antibody (Sigma); rabbit polyclonal anti-Rab11 antibody (Santa Cruz Biotechnology); and rabbit polyclonal anti-synaptophysin (DAKO).

Histopathological analyses for DM-associated pathology

Most of the tissues were fixed in 10% neutral buffered formalin, processed routinely and stained with hematoxylin and eosin (HE) for histopathological analyses. The pancreases were also stained with direct fast scarlet (DFS; Muto) for identification of islet amyloid.

Immunohistochemistry

Brain samples were immersion-fixed in 10% neutral buffered formalin, embedded in paraffin, and cut into 4 μm-thick sections. For immunohistochemical analyses with anti-GAβ antibody, brain samples were fixed in 4% paraformaldehyde. Sections were deparaffinized by pretreatment with 0.5% periodic acid, and then incubated overnight at 4°C free floating in the following primary antibody solutions: (1) Aβ (1:100); (2) APP (1:100); (3) Rab5 (1:100); (4) GAβ (1:20); or (5) AT8 (1:100). Following brief washes with buffer, the sections were sequentially incubated with biotinylated goat anti-mouse IgG (1:200) or goat anti-rabbit IgG (1:200), followed by streptavidin-biotin-horseradish peroxidase complex (DAKO). Immunoreactive elements were visualized by treating the sections with 3–3' diaminobenzidine tetroxide (Dojin Kagaku). The sections were then counterstained with hematoxylin. The immunoreactivity of Aβ, GAβ, APP or Rab5 in a given cortical area was quantified with computer software Image J 1.49i (National Institue of Health). For quantification analyses, the sections were not counterstained with hematoxylin.

Biochemical analyses of monkey brains

Frozen monkey brain tissue (wet weight 0.2 g) was homogenized in a glass homogenizer with 4 ml of homogenate buffer solution (0.32 M sucrose, 10 mM Tris-HCl [pH 7.6], 0.25 mM PMSF, and 1 mM EDTA, and Complete Mini proteinase inhibitor cocktail), and then centrifuged at 100,000xg for 20 min to obtain the supernatant fraction. The proteins in the fraction were subjected to dot blot analyses. Brain homogenates were also centrifuged at 1,000×g for 10 min to remove the nuclear fraction, and then the supernatant was centrifuged at 105,000×g for 60 min to obtain the microsomal fraction. The proteins in the microsomal fraction were subjected to Western blot analyses. For Aβ ELISA, brain homogenates were incubated with Triton-X100 at a final concentration of 1% for 15 min at 37°C, and spun at 100,000 × g for 20 min at 20°C. The pellet was homogenized in homogenate buffer containing 1% sarkosyl, incubated for 15 min at 37°C, and spun at 100,000 × g for 20 min at 20°C. The sarkosyl-insoluble pellet was sonicated in 70% folic acid, cleared by centrifugation at 100,000 × g for 20 min at 20°C. The supernatant was evaporated, and then resuspended in dimethyl sulfoxiside (Sigma).

Dot blot analyses

Dot blot analyses were performed to assess age- and DM-related changes in GAβ formation. Brain samples were adjusted to 1 mg, 2.5 mg, and 5 mg, and then applied onto nitrocellulose membranes and dried. The membranes were blocked with 5% nonfat dried milk in 20 mM PBS (pH 7.0) and 0.1% Tween-20 for 1 h at room temperature, and then incubated in the anti-GAβ antibody solution overnight at 4°C. They were then incubated with horseradish peroxidase-conjugated goat anti-mouse IgG (1:10000; Cell Signaling Technology) for 1 h at room temperature. Immunoreactive elements were visualized using enhanced chemiluminescence (Luminata Forte Western HRP Substrate, Millipore).

Western blot analyses

Western blot analyses were performed to assess age- and DM-related changes in APP, Rab5, Rab7, Rab11, DHC, DIC, KHC, KLC, NEP, Cathepsin D heavy chain (CatD HC), and LC3 expression. Each microsome fraction prepared as described above was adjusted to 5 mg, and then analyzed using SDS-polyacrylamide gel electrophoresis using 14% (for LC3) or 12.5% (other proteins) acrylamide gels. Separated proteins were blotted onto polyvinylidense fluoride membranes (Immobilon P; Millipore). The membranes were blocked with 5% nonfat dried milk in

20 mM PBS (pH 7.0) and 0.1% Tween-20 for 1 h at room temperature, and then incubated overnight at 4°C in the following primary antibody solutions: (1) synaptophysin (1:20000); (2) APP (1:2000); (3) Rab5m (1:2000); (4) Rab7 (1:10000); (5) Rab11 (1:2000); (6) DHC (1:1000); (7) DIC (1:20,000); (8) KHC (1:5,000); (9) KLC (1:1000); (10) NEP (1:4,000); (11) CatD (1:2,000); or (12) LC3 (1:2,000). They were then incubated with either horseradish peroxidase-conjugated goat anti-mouse IgG or goat anti-rabbit IgG (1:10,000; Cell Signaling Technology) for 1 h at room temperature. Immunoreactive elements were visualized using enhanced chemiluminescence. To confirm reproducibility, immunoreactive bands obtained from the Western blots were quantified using commercially available software (Quantity One; PDI, Inc.).

Aβ ELISA

Total Aβ levels in young monkey, normal adult monkey, DM-affected monkey, and normal aged monkey brains were determined using a sandwich ELISA. The kit for Aβ (1-X) was obtained from IBL (Gunma, Japan). The ELISA assay was carried out according to the instruction manual. All samples were measured in duplicate.

Data analyses

Data obtained from quantitative analyses of immunohistochemistry and biochemical analyses are shown as means ± SD. For statistical analyses, one-way ANOVAs were performed, followed by the Fisher's post hoc test.

Results

Clinical background and DM-associated pathology in cynomolgus monkeys

Tsukuba Primate Research Center (TPRC) maintains a large breeding and rearing colony of cynomolgus monkeys for high-quality production of nonhuman primate models and biomedical investigations. In the TPRC colony, some adult monkeys are spontaneously affected with type 2 DM for various reasons, such as pregnancy history and environmental factors. The clinical background of all monkeys used for this study is shown in (S1 Table). TPRC has accumulated clinical data for more than 40 years. Based on these data, the normal blood glucose level for female monkeys is in the range of 24 to 74 mg/dL, and for male monkeys the range is 24 to 76 mg/dL. Normal blood triglyceride levels are in the range of 8 to 85 mg/dL for females, and 6 to 52 mg/dL for males. The blood glucose and triglyceride levels of normal adult monkeys used in the present study were all in the normal range, and their body weights were in the range of historical TPRC data for normal monkeys (S1 Table). All DM-affected monkeys, on the other hand, exhibited hyperlipidemia and hyperglycemia (S1 Table). These DM-affected monkeys were severely obese; however, their body weight at acquisition of their brains for this study had decreased to about less than half the maximum body weights they attained during their lifetime (S1 Table).

Histopathologically, islet amyloid was found in the pancreases of all DM-affected adult monkeys (Fig. 1A). In eight DM cases, most hyalinized islets were replaced with severe amyloid deposits, with the remaining islet cells being severely degenerated or decreased in apparent number (Fig. 1A-C). The hyalinized islets with severe amyloid deposits stained positive for direct fast scarlet (DFS) (Fig. 1D). Furthermore, two DM cases had fatty degeneration of the liver, and one DM case had mild atheromatosis. Thus, histopathological analyses demonstrated that these adult monkeys clearly had DM. On the other hand, we did not observe apparent vascular lesions in all DM monkey brains.

DM accelerates Aβ pathology in cynomolgus monkey brain

Next, we conducted immunohistochemical analyses to assess whether DM affects AD pathology in these cynomolgus monkey brains. As previously reported [26, 36], we observed SP depositions in the brains of aged monkeys (Fig. 2A), but not in those of normal adult monkeys younger than 20 years of age (Fig. 2B-D). Strikingly, we apparently observed diffuse Aβ-immunopositive SPs in brains of six DM-affected adult monkeys younger than 20 years old, even though they were very small quantities as compared to aged monkey brains (Fig. 2E-I). In aged cynomolgus monkey brains, cerebral amyloid angiopathy (CAA) lesions are also observed, and NFTs are observed over 32-year-old monkey brains [26, 27]. Although abnormally phosphorylated tau accumulation was not observed, we found much severe CAA in the brains of aged monkeys with DM (Fig. 3).

DM enhances GAβ generation in adult monkey brains

To assess whether DM affects Aβ level in monkey brains, we examined Aβ ELISA analyses. In aged monkey brains, Aβ level was significantly increased, suggesting that the increase of Aβ level correlates with age-dependent SP depositions (Fig. 4A). However, surprisingly, Aβ level was just slightly increased in DM-affected adult monkey brains as compared to normal adult monkey brains (Fig. 4A). We previously identified a unique Aβ species, called GAβ, characterized by its binding to GM1 ganglioside; GAβ was demonstrated in brain tissue along with early pathological changes characteristic of AD [32]. Accumulating evidence suggests that GAβ accelerates Aβ fibril formation by acting as a seed molecule [37–40]. We have also confirmed age-dependent GAβ generation in cynomolgus monkey brains [32, 41].

To test our hypothesis that DM enhances GAβ generation in the brain, we performed additional immunohistochemical analyses using an anti-GAβ-specific antibody. In the brains of normal adult monkeys, we observed little, if any, immunoreactivity with anti-GAβ antibody (Fig. 4B). In contrast, in the brains of DM-affected adult monkeys, we frequently observed neurons clearly immunopositive for anti-GAβ antibody (Fig. 4B). Quantitative analyses also confirmed that the immunoreactivity of GAβ was significantly increased in DM-affected adult monkey brains (Fig. 4C).

For biochemical analyses, we carried out dot blot analyses on monkey brain samples. Because of its conformational features, GAβ is not recognized by western blot analyses. Our dot blot analyses showed that GAβ generation increased in an age-dependent manner in cynomolgus monkey brains (Fig. 4D). GAβ immunoreactivity was much stronger in aged monkey brains, indicating that the amount of GAβ generated generally parallels age-dependent SP deposition as well as Aβ level. In normal adult monkey brains, the amount of GAβ generation was not much different from that in young monkey brains (Fig. 4D). It is noteworthy that GAβ generation was significantly increased in DM-affected adult monkey brains (Fig. 4E).

DM exacerbates endocytic disturbance with significant increase of Rab GTPases

In the brains of early-stage AD patients, neuronal endocytic pathology, such as intracellular accumulation of abnormally enlarged endosomes, is frequently observed [42–44]. We previously demonstrated that aging causes endocytic pathology along with a significant increase in Rab GTPases, resulting in the intracellular accumulation of APP [45]. This endocytic disturbance was observed in brains from cynomolgus monkeys almost 10 years before SP deposition begins [46]. We also reported that GAβ accumulates in enlarged endosomes of neurons in aged cynomolgus monkey brains [33]. Moreover, endocytic disturbance induces GAβ generation [34].

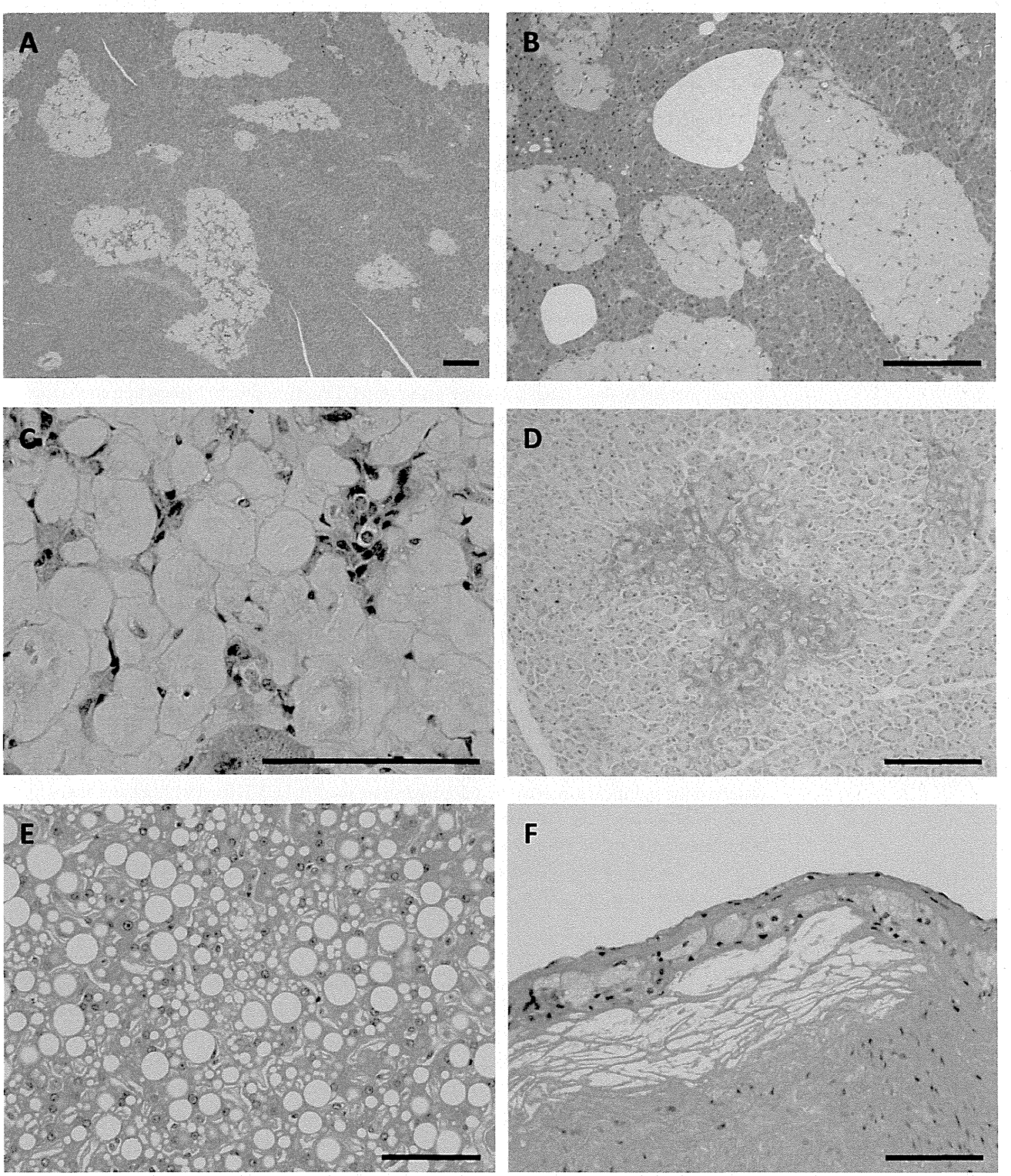

Fig 1. Histopathology of adult monkeys with type 2 diabetes mellitus. (A) Hematoxylin-eosin (HE)-stained section of the pancreas from a 17-year-old cynomolgus monkey with type 2 diabetes mellitus (DM) (S1 Table, Number 1). Most of the islets were replaced by abundant amyloid deposits. (B) HE-stained section of the pancreas from an 18-year-old cynomolgus monkey with DM (S1 Table, Number 3). Most of the islets were replaced with severe amyloid deposits. (C) HE-stained section of the pancreas from a 19-year-old cynomolgus monkey with DM (S1 Table, Number 7) showing hyalinized islets. Very few

islet cells remain. (D) Direct fast scarlet-stained section of pancreas from an 18-year-old cynomolgus monkey with DM (S1 Table, Number 5). Hyalinized islets with severe amyloid deposition were positive for direct fast scarlet staining. (E) HE-stained section of the liver from an 18-year-old cynomolgus monkey with DM (S1 Table, Number 3). Marked fatty degeneration was observed in the liver. (F) HE-stained section of the aorta from an 18-year-old cynomolgus monkey with DM (S1 Table, Number 5). Mild atheromatosis with foam cells and sterol clefts was observed in the aorta. Scale bars for a-f, 100 μm.

doi:10.1371/journal.pone.0117362.g001

Taken together, these findings suggest that endocytic disturbance is involved in age-dependent Aβ pathology. Thus, to assess whether DM enhances endocytic disturbance, we investigated endocytic pathology in monkey brains.

In the brains of normal adult monkeys, APP and Rab5-positive early endosomes were observed as small granules in neurons (Fig. 5A, B). By contrast, in the brains of DM-affected adult monkeys, the immunoreactivity of APP and Rab5 was significantly stronger and the immunopositive granules were larger (Fig. 5C, D). Quantitative analyses confirmed that both APP- and Rab5-immunopositive granules were significantly increased in DM-affected adult monkey brains as compared to normal adult monkey brains (Fig. 5E). Western blot analyses showed that Rab5, Rab7 (late endosome-associated GTPase), and Rab11 (recycling endosome-associated GTPase) were increased in aged monkey brains, corroborating that age-dependent endocytic disturbance does occur in monkey brains, as previously reported (Fig. 5F, G) [45]. The amount of APP was also significantly increased in aged monkey brains as previously reported (Fig. 5F, G) [45, 47]. In the brains of DM-affected adult monkeys, Rab GTPases and APP levels were apparently increased compared to the brains of normal adult monkeys, being almost same as in aged monkey brains (Fig. 5F, G).

DM affects cathepsin D level and autophagosome clearance

Endosome trafficking is mediated by axonal transport motor proteins [48], and a recent study showed that the experimental induction of DM alters axonal motor protein levels in rodent model [49]. In the present study, we did not find apparent differences in axonal motor protein levels between normal and DM-affected adult monkey brains (Fig. 6). Endocytic disturbance is also induced by the breakdown in lysosomal degradation [50]. In DM-affected adult monkey brains, the level of cathepsin D (CatD) heavy chain increased (Fig. 6). On the other hand, we observed the significant increase in autophagosome marker LC3-II level without any alterations in LC3-I level (Fig. 6). A recent study also showed that DM-associated down-regulation of insulin signals reduces the level of Aβ degrading enzymes such as neprilysin (NEP) [51]. However, we did not find a clear reduction tendency in NEP levels in the brains of DM-affected adult monkeys (Fig. 6).

Discussion

Here, we present the evidence that DM accelerates Aβ pathology in the brain parenchyma of nonhuman primates, which have not undergone any genetic manipulation. We demonstrated that DM does so by enhancing the generation of GAβ, the endogenous seed for Aβ fibril formation in the brain. The brains of DM-affected adult monkeys contained robust endocytic pathology, such as a significant increase in Rab GTPases and intraneuronal accumulation of enlarged endosomes. Endocytic disturbance is a cellular pathological characteristic of neurons of AD patients and enhances GAβ generation [33, 34]. Thus, our present findings suggest that DM exacerbates age-dependent endocytic disturbance, which in turn enhance GAβ generation resulting in accelerated Aβ pathology.

Recent epidemiological/clinical studies suggest that DM is a major risk factor for developing AD [5–9]. However, the underlying mechanisms for this association remain unclear. Thus, in the present study, we performed histopathological and biochemical analyses using brains from

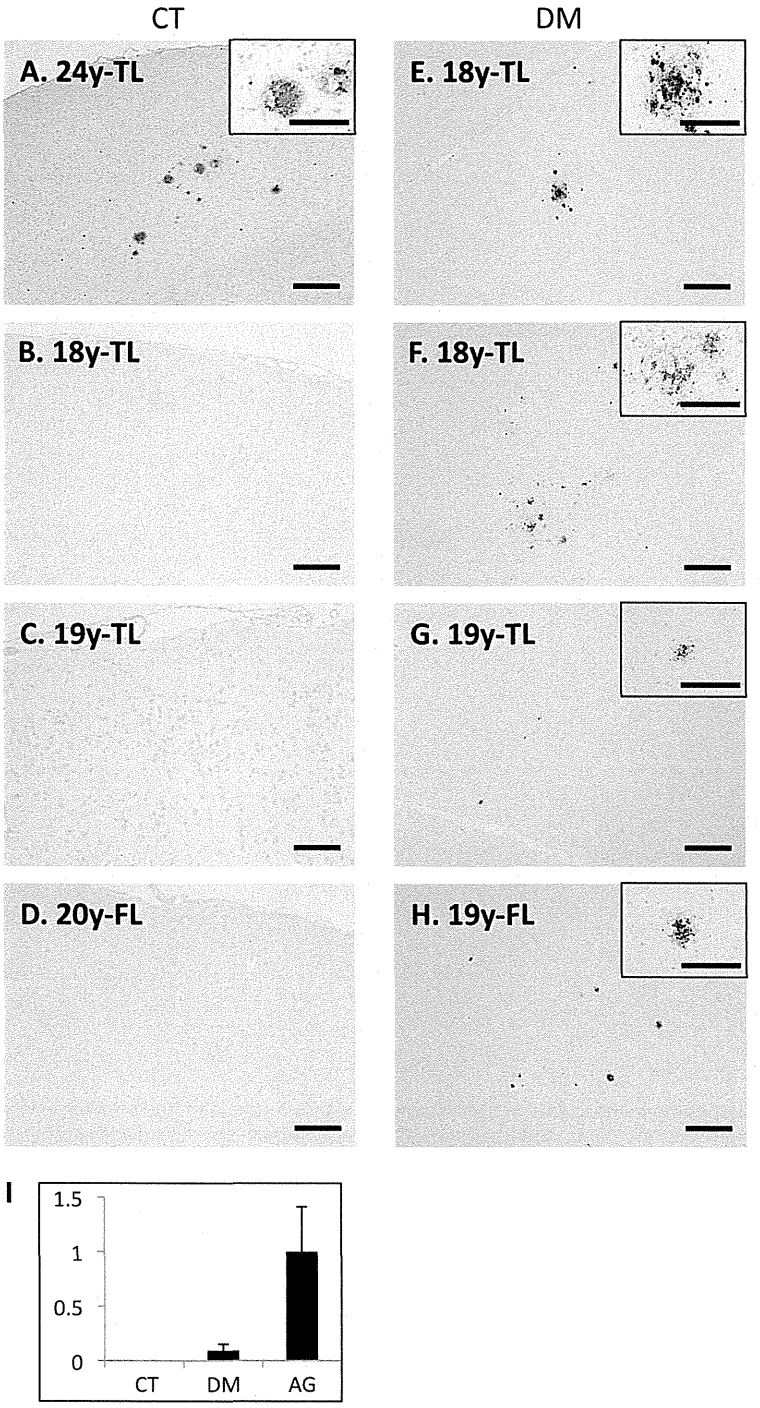

Fig 2. Senile plaques in the brains of adult monkeys with DM. Images of temporal lobe (TL) and frontal lobe (FL) sections from normal cynomolgus monkeys (A-D) and cynomolgus monkeys with DM (E-H). Sections were immunostained with anti-Aβ antibody and counterstained with hematoxylin. In aged monkey brains, we observed SPs immunostained with anti-Aβ antibody, as previously reported (A). In contrast, we did not observe Ab-immunopositive structures in the normal adult monkey brains (B-D). However, we did observe small but obvious Aβ-immunopositive senile plaques (SPs) in the frontal and temporal cortices of DM-affected adult monkeys (E-H). Scale bars, 100 μm. (I) Quantitative image analysis of Ab-immunopositive area in the sections obtained from female normal adult monkey, DM-affected adult monkey, and normal aged monkey brains. Data obtained from normal aged monkey brains were set as standards. Y-axes show the mean values of the quantified data. CT, normal cynomolgus monkeys. DM, DM-affected monkeys.

doi:10.1371/journal.pone.0117362.g002

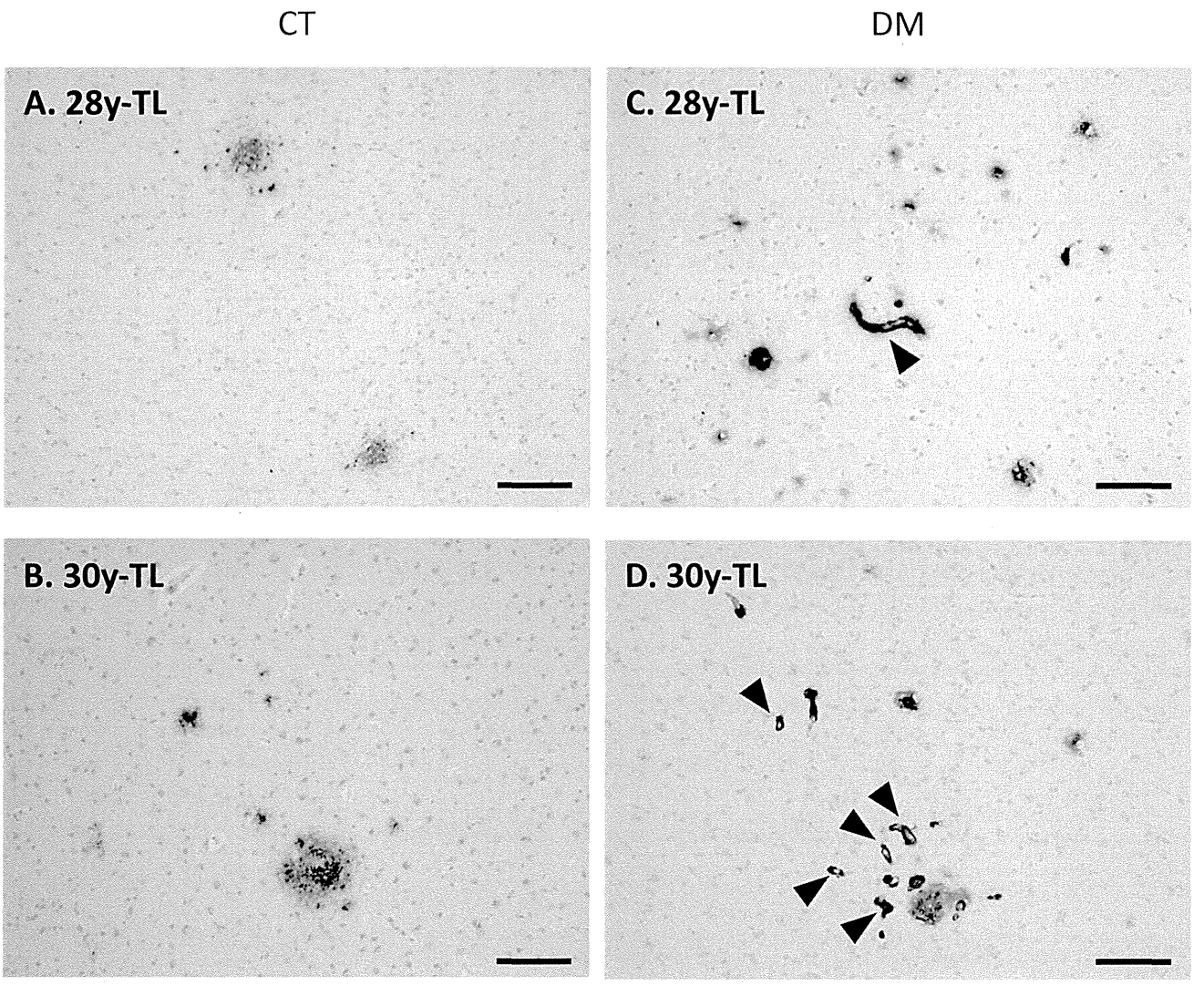

Fig 3. Cerebral amyloid angiopathy in the brains of aged monkeys with DM. Images of temporal lobe (TL) sections from normal cynomolgus monkeys (A, B) and cynomolgus monkeys with DM (C, D). Sections were immunostained with anti-Aβ antibody and counterstained with hematoxylin. In the brains of DM-affected aged monkeys, we observed very severe CAA lesions (arrowheads) as compared to normal aged monkeys. CT, normal aged monkeys. DM, DM-affected aged monkeys. Scale bars, 100 μm.

doi:10.1371/journal.pone.0117362.g003

DM-affected cynomolgus monkeys in order to assess the relationship between DM and AD pathology. As previously reported, SPs spontaneously form in the brains of aged monkeys over the age of 25 years, but never in the brains of normal young monkeys and adult monkey younger than 20 years (Fig. 2A-D) [26]. Strikingly, our immunohistochemical analyses revealed SP depositions in the brains of DM-affected adult monkeys as young as 18 years (Fig. 2E-H). To our knowledge, this is the first study to show that DM enhances Aβ pathology even in nonhuman primate brains without genetic manipulation. We also observed much severe CAA lesions in the brains of DM-affected aged monkeys than in those of normal aged monkeys (Fig. 3). These findings are consistent with the previous studies showing that DM-related conditions induce amyloidogenesis and Aβ pathology in rodent models [14–25]. Although additional